Disclaimer

This Report, including the data and information contained in this Report, is provided to you on an "as is" and "as available" basis at the sole discretion of the Government of Alberta and subject to the terms and conditions of use below (the "Terms and Conditions"). The Government of Alberta has not verified this Report for accuracy and does not warrant the accuracy of, or make any other warranties or representations regarding, this Report. Furthermore, updates to this Report may not be made available. Your use of any of this Report is at your sole and absolute risk.

This Report is provided to the Government of Alberta, and the Government of Alberta has obtained a license or other authorization for use of the Reports, from:

> Shell Canada Energy, Chevron Canada Limited. and Marathon Oil Canada Corporation, for the Quest Project
>
> (collectively the "Project")

Each member of the Project expressly disclaims any representation or warranty, express or implied, as to the accuracy or completeness of the material and information contained herein, and none of them shall have any liability, regardless of any negligence or fault, for any statements contained in, or for any omissions from, this Report. Under no circumstances shall the Government of Alberta or the Project be liable for any damages, claims, causes of action, losses, legal fees or expenses, or any other cost whatsoever arising out of the use of this Report or any part thereof or the use of any other data or information on this website.

Terms and Conditions of Use

Except as indicated in these Terms and Conditions, this Report and any part thereof shall not be copied, reproduced, distributed, republished, downloaded, displayed, posted or transmitted in any form or by any means, without the prior written consent of the Government of Alberta and the Project.

The Government of Alberta's intent in posting this Report is to make them available to the public for personal and non-commercial (educational) use. You may not use this Report for any other purpose. You may reproduce data and information in this Report subject to the following conditions:

- any disclaimers that appear in this Report shall be retained in their original form and applied to the data and information reproduced from this Report
- the data and information shall not be modified from its original form
- the Project shall be identified as the original source of the data and information, while this website shall be identified as the reference source, and
- the reproduction shall not be represented as an official version of the materials reproduced, nor as having been made in affiliation with or with the endorsement of the Government of Alberta or the Project

By accessing and using this Report, you agree to indemnify and hold the Government of Alberta and the Project, and their respective employees and agents, harmless from and against any and all claims, demands, actions and costs (including legal costs on a solicitor-client basis) arising out of any breach by you of these Terms and Conditions or otherwise arising out of your use or reproduction of the data and information in this Report.

Your access to and use of this Report is subject exclusively to these Terms and Conditions and any terms and conditions contained within the Report itself, all of which you shall comply with. You will not use this Report for any purpose that is unlawful or prohibited by these Terms and Conditions. You agree that any other use of this Report means you agree to be bound by these Terms and Conditions. These Terms and Conditions are subject to modification, and you agree to review them periodically for changes. If you do not accept these Terms and Conditions you agree to immediately stop accessing this Report and destroy all copies in your possession or control.

These Terms and Conditions may change at any time, and your continued use and reproduction of this Report following any changes shall be deemed to be your acceptance of such change.

If any of these Terms and Conditions should be determined to be invalid, illegal or unenforceable for any reason by any court of competent jurisdiction then the applicable provision shall be severed and the remaining provisions of these Terms and Conditions shall survive and remain in full force and effect and continue to be binding and enforceable.

These Terms and Conditions shall: (i) be governed by and construed in accordance with the laws of the province of Alberta and you hereby submit to the exclusive jurisdiction of the Alberta courts, and (ii) ensure to the benefit of, and be binding upon, the Government of Alberta and your respective successors and assigns.

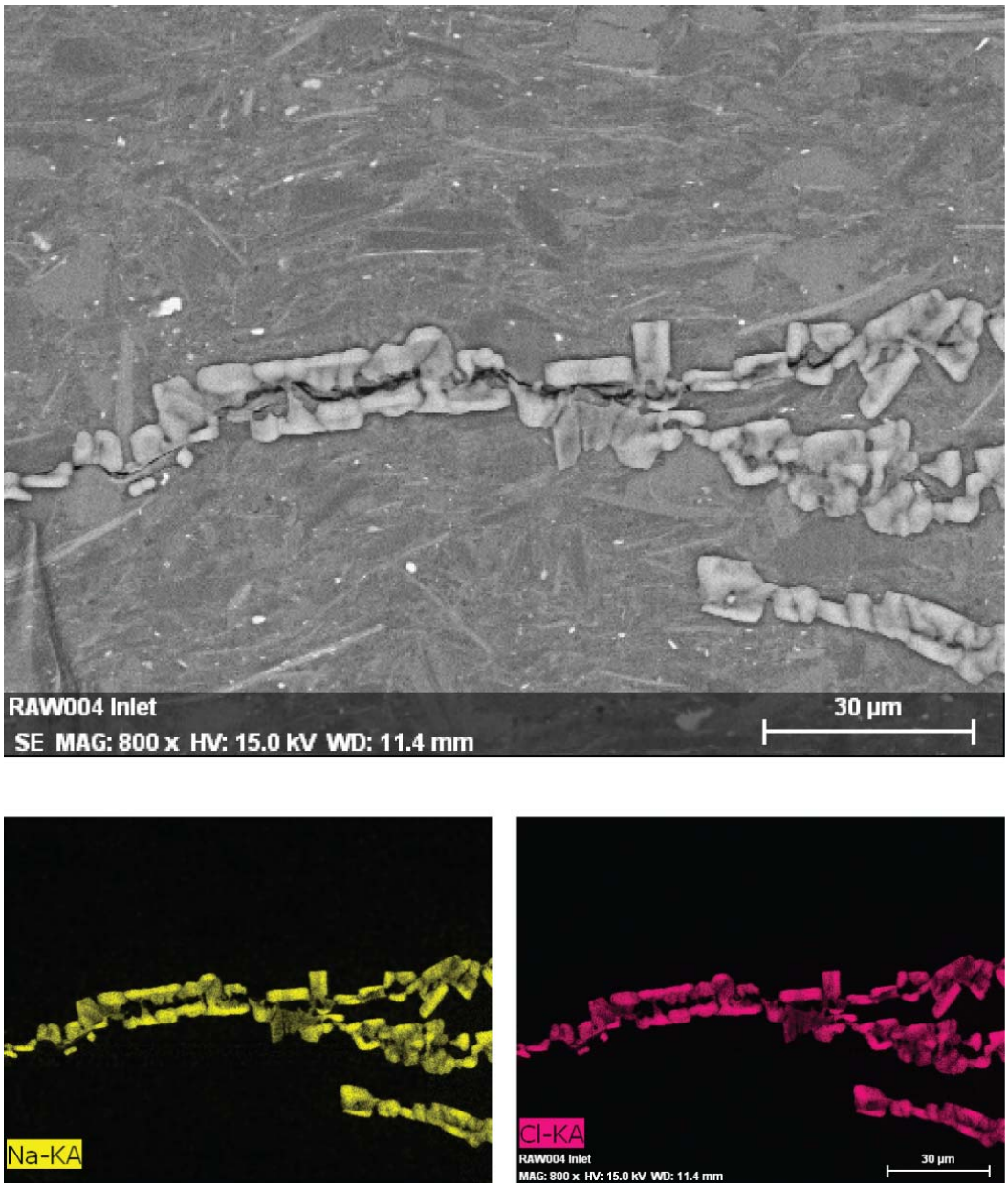

Figure 4.7: **Top: SEM image taken on the top surface of RAW004 inlet disk after SC CO_2 entry pressure measurements. Bottom: elemental mapping on the above image for Na and Cl.**

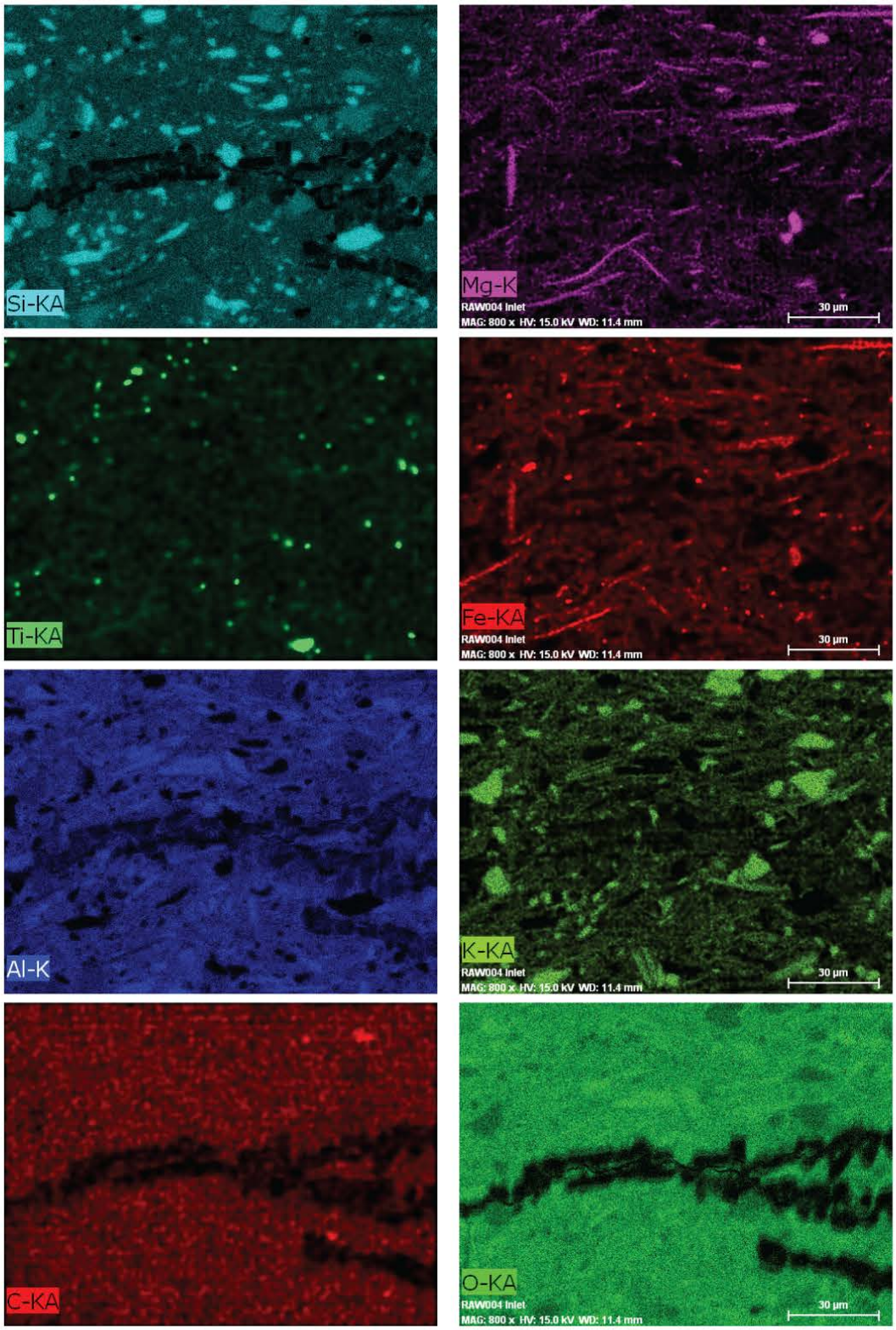

Figure 4.8: Elemental mapping on the SEM image in Figure 4.7 for other major elements.

Figure 4.9: SEM image taken on the top surface of RAW004 middle disk after SC CO_2 entry pressure measurements.

Table 4.2: Elemental Analysis on the Image in Figure 4.9

Element	Atom	Mass	Error
	at.%	wt.%	wt.%
Carbon ('C)	18.34	11.66	5.5
Oxygen (O)	56.31	47.69	18.9
Sodium (Na)	0.72	0.87	0.1
Magnesium (Mg)	1.07	1.38	0.1
Aluminum (Al)	7.96	11.38	0.7
Silicon (Si)	11.73	17.44	1.0
Phosphorus (P)	0.14	0.24	0.0
Sulfur (S)	0.06	0.11	0.0
Chlorine (Cl)	0.09	0.17	0.0
Potassium (K)	1.58	3.27	0.2
Titanium (Ti)	0.24	0.61	0.0
Iron (Fe)	1.75	5.18	0.2

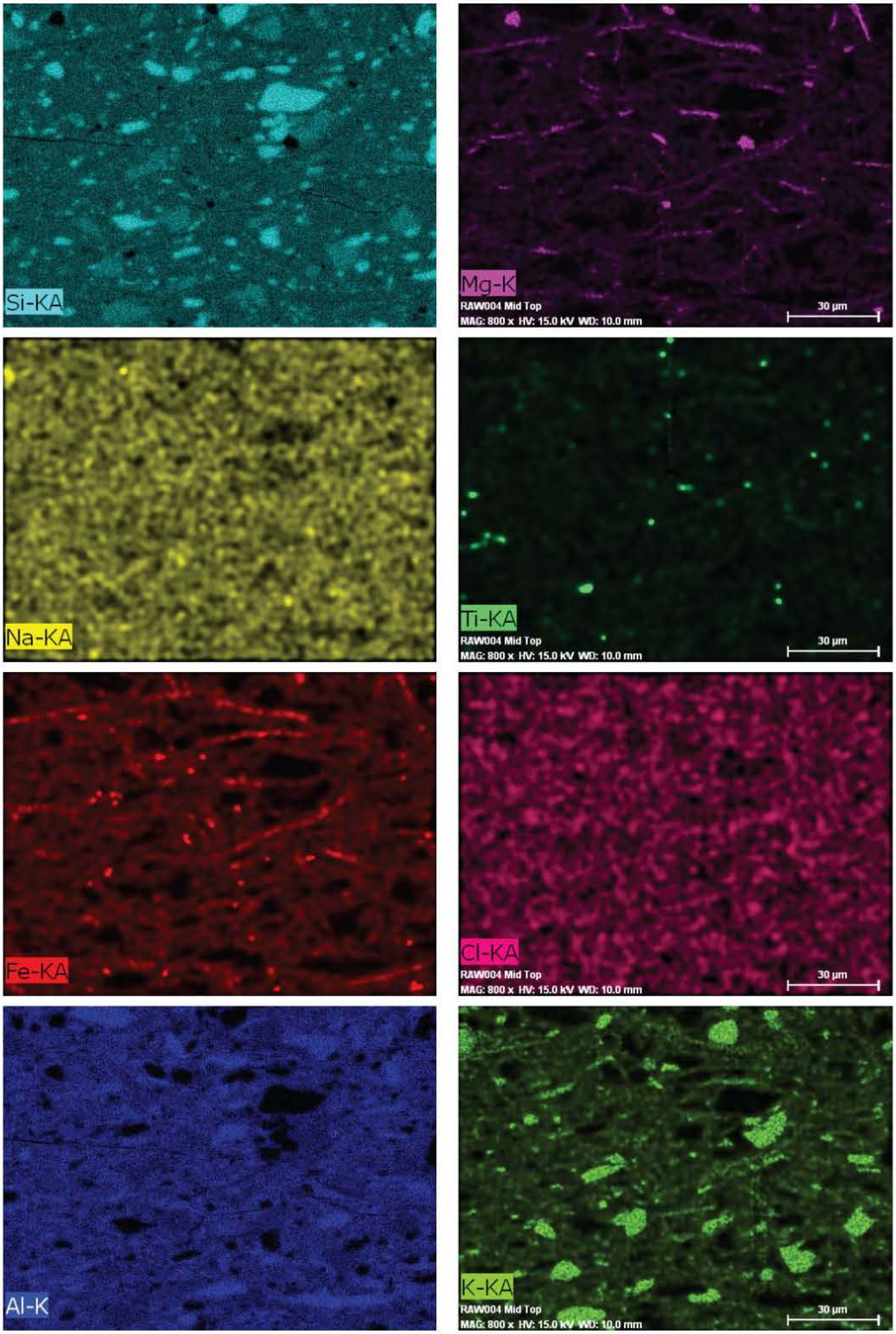

Figure 4.10: Elemental mapping on the SEM images in Figure 4.9 for major elements.

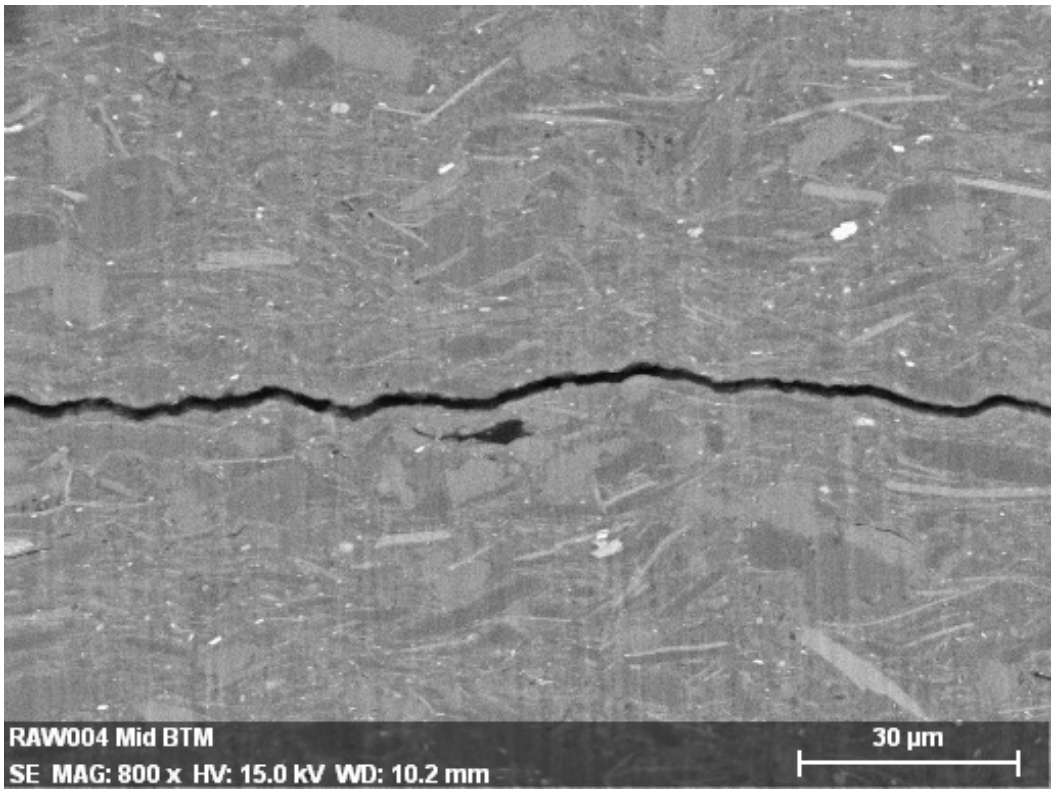

Figure 4.11: SEM image taken on the bottom surface of RAW004 middle disk after SC CO_2 entry pressure measurements.

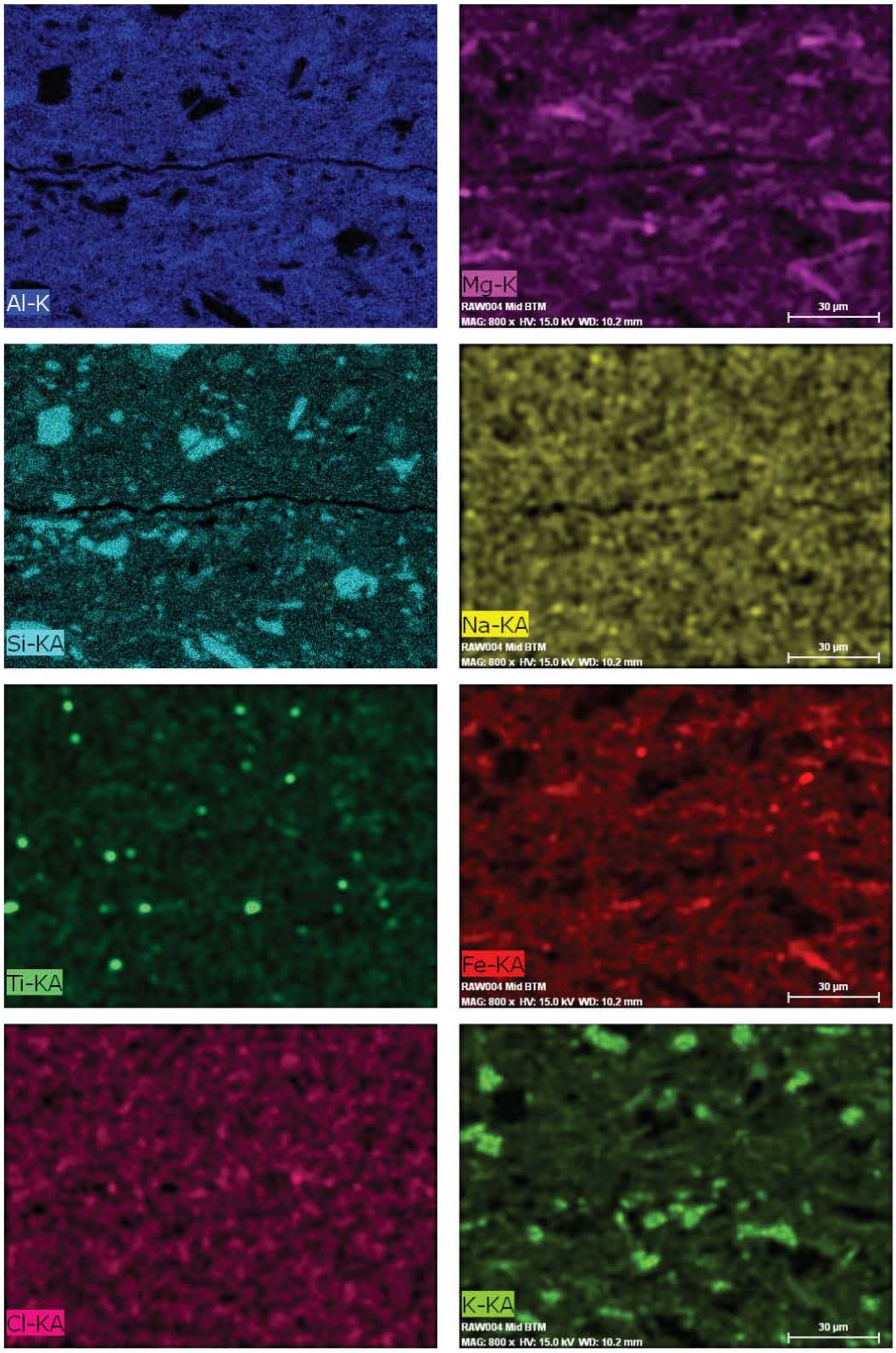

Figure 4.12: Elemental mapping on the SEM images in Figure 4.11 for major elements.

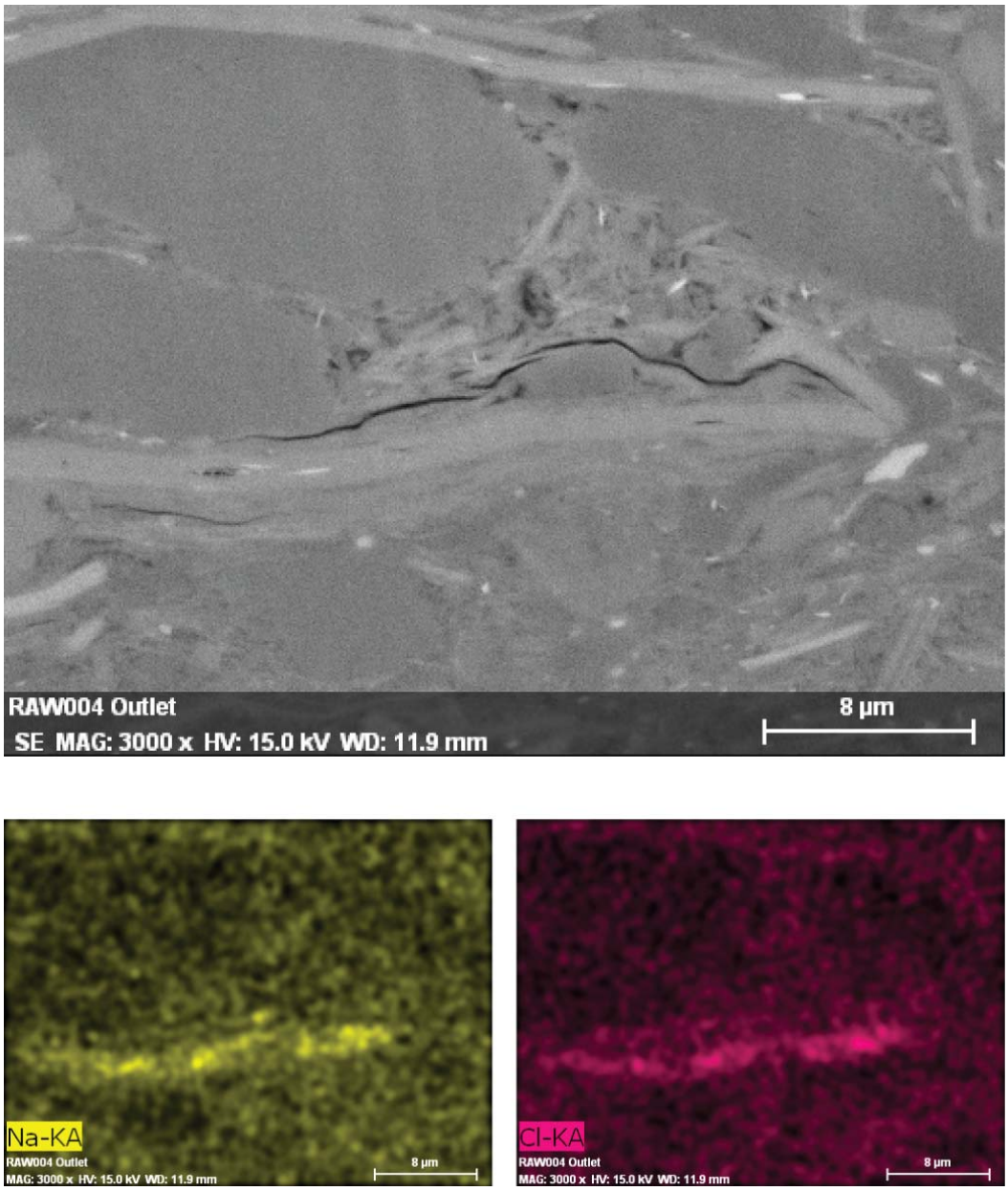

Figure 4.13: **Top: SEM image taken on the top surface of RAW004 outlet disk after SC CO_2 entry pressure measurements. Bottom: elemental mapping on the above image for Na and Cl.**

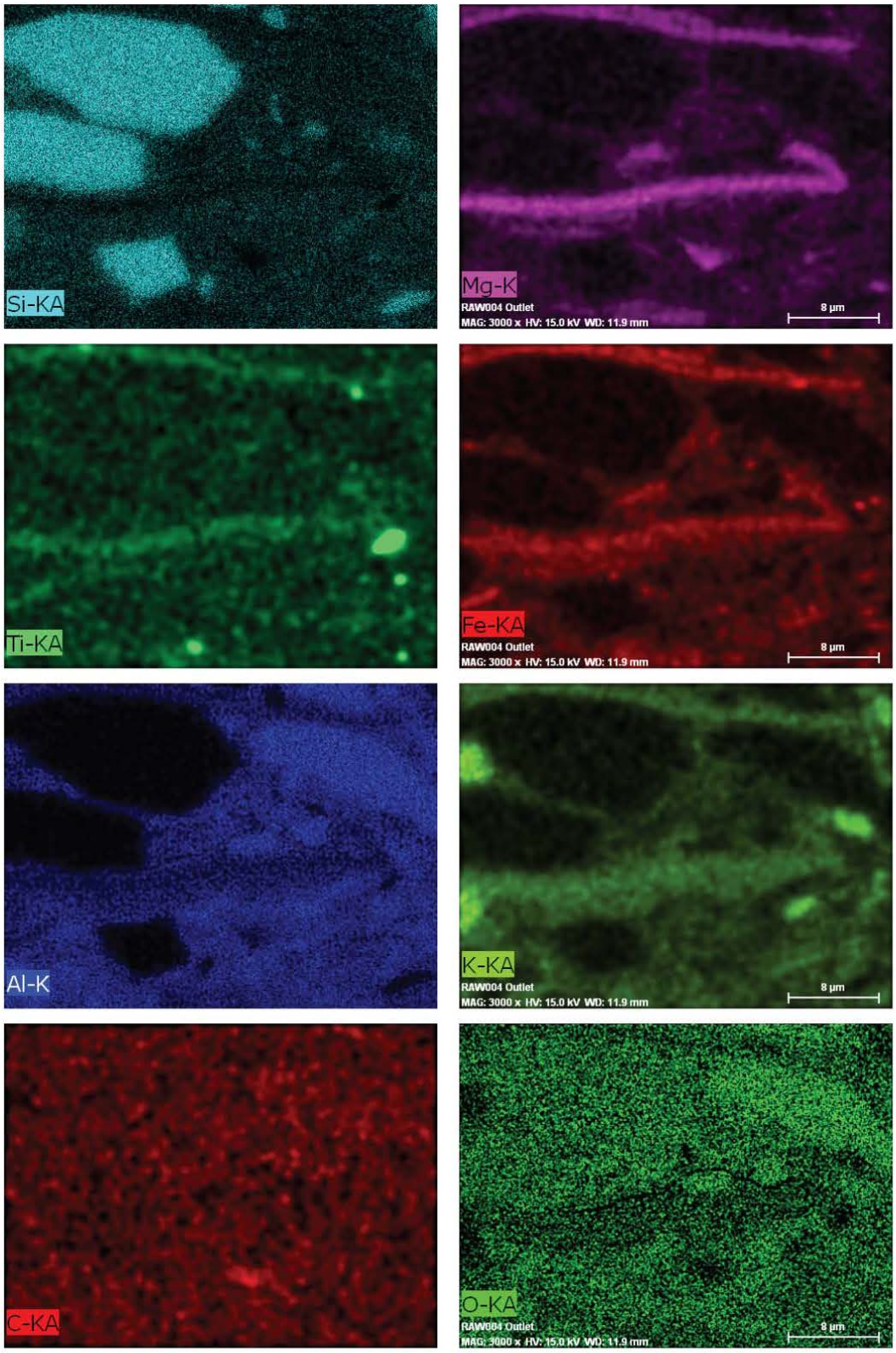

Figure 4.14: Elemental mapping on the SEM images in Figure 4.13 for other major elements.

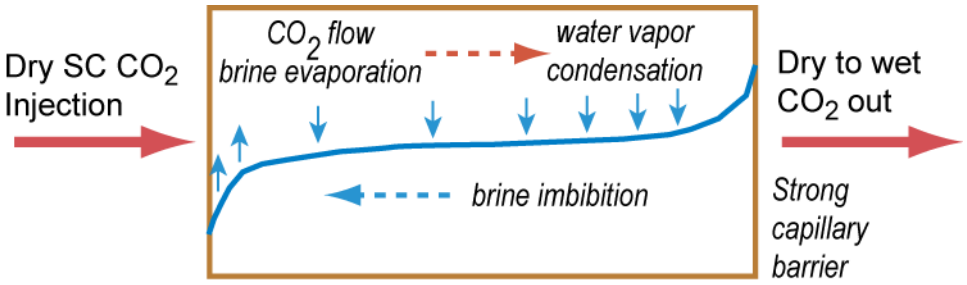

Figure 4.15: A conceptual model of CO_2-brine interaction during CO_2 injeciton.

From the above image study, halite crystals were found along the edges of cracks close to the inlet of RAW004 after the SC CO_2 entry pressure measurement. The portion of core sample away from the inlet appeared to be similar to that before the CO_2 entry pressure test in both image and elemental analysis; no halite was observed. The halite crystals were probably due to the SC CO_2-brine-rock interaction that is conceptually demonstrated in Figure 4.15. As dry SC CO_2 enters the rock, there can be two flows in opposite directions. At the upstream, dry SC CO_2 displaces the brine and vaporizes water in the brine. The evaporation concentrates the brine and leads to salt precipitation. Water is carried by CO_2 and moves downstream in the vapor phase. The evaporation can reduce the local water saturation below the equilibrium saturation for the applied capillary pressure (CO_2 injection pressure minus local water phase pressure). Water can consequently re-imbibe towards the inlet, ie. water moves upstream in the liquid phase. As CO_2 pressure drops, water may also recondenses from the CO_2 near the outlet and dilutes the brine. This evaporation/condensation/imbibition cycle can transport additional salt towards the inlet. Therefore, halite precipitation should happen close to the inlet side. The dry-out and salt precipitation have been studied through coreflood experiments and numerical modeling [10] [11] [12] [13] [14].

Table 4.3: X-ray Diffraction Bulk Analysis on RAW004 after Entry Pressure Test

Disk	Illite	Kaolinite	Chlorite-Fe	Calcite	Pyrite	K-Feldspar	Quartz
Inlet	27 (8)	24 (7)	5 (2)	6 (1)	3 (2)	6 (2)	29 (4)
Middle	20 (7)	22 (7)	5 (2)	10 (2)	4 (2)	7 (2)	32 (4)
Outlet	30 (9)	25 (8)	3 (2)	2 (1)	4 (2)	10 (3)	27 (4)

Results from XRD analysis on those three disks are summarized in Table 4.3 and Table 4.4, where the numbers in parentheses represent the estimated standard deviations at the 95% confidence level in unit of weight percent. Also note that the Clay Isolate Fraction analysis only covered those clay minerals with particle sizes from 0.26 to 4.7 microns. Both bulk and clay analysis suggested that the three disks from RAW004 had similar mineral compositions within the uncertainty range except for calcite. From Table 4.3, calcite was about 6 wt% in the inlet disk, 10 wt% in the middle disk, and 2 wt% in the outlet disk, respectively. The variation among disks appeared to be bigger than estimated

uncertainties. In comparison, no calcite was identified on the end-trim of RAW004 before the entry pressure test.

Table 4.4: X-ray Diffraction Analysis on Clay Isolate Fraction Components on RAW004 after Entry Pressure Test

Disk	Illite	Kaolinite	Chlorite - Fe
Inlet	45 (14)	51 (14)	3 (3)
Middle	48 (14)	49 (14)	3 (3)
Outlet	45 (14)	51 (14)	4 (3)

Precipitation of calcite highlighted the potential cation exchange followed by another SC CO_2-brine-rock interaction in pore space as listed below:

$$CO_2 + H_2O = H_2CO_3 = H^+ + HCO_3^- \quad (4.1)$$

$$CaCO_3 + H_2CO_3 = Ca^{2+} + 2HCO_3^-. \quad (4.2)$$

Moreover, it also suggested that the dominant process for CO_2 invading into RAW004 was diffusion instead of viscous flow. Generally the calcite dissolution/precipitation strongly depends on the pH value of the environment, which is in turn strongly impacted by the CO_2 partial pressure. If viscous flow occurred in the pore space, as SC CO_2 was continuously injected into the pore space, the formation brine would have been strongly acidified with pH as low as 5 [3]. Calcite precipitation would be much less possible in such an acid solution.

From the above XRD analysis, an order-of-magnitude estimation can be made on the effective CO_2 diffusion coefficient in the cap rock. Total precipitated calcite was estimated to be about 1 g or 0.01 mol, where weight of the three disks from RAW004 was estimated from the bulk volume and an approximate bulk density of 2.7 g/cc. Reactions in Eq. (4.1) and (4.2) showed that 2 mole of CO_2 is needed to generate 1 mole of calcite. The average CO_2 flux during the 673-hour measurement was about 6.5×10^{-6} mol/(cm^2 hr). On the other hand, formation brine in the inlet face of RAW004 was assumed to be fully saturated with CO_2 as it was in direct contact with SC CO_2 during the test. Under the measurement conditions, solubility of CO_2 was about 61.3 scf/stb or 10.8 cc/cc. So the molar concentration of CO_2 was 4.6×10^{-4} mol/cm^3. At the outlet side, the amount of calcite was very low according to the XRD result, which suggested that the CO_2 diffusion front had not reached the outlet yet. CO_2 concentration should be close to the original value and was much lower compared to that at the inlet. The concentration gradient of CO_2 across the core plug with its outlet concentration ignored was about 3.4×10^{-4} mol/cm^4. If its porosity was assumed to be 2%, an effective diffusion coefficient for CO_2 in RAW004 was estimated to be 3×10^{-4} cm^2/s.

Note that calcium was not observed in the EDS spectrum on samples from those disks. This was possibly due to the process of Ar milling for sample preparation. One crushed sample after XRD was analyzed by EDS again and calcium was clearly identified. More study may be required to assess this issue.

5. Conclusion and Recommendation on Future Study

In conclusion, capillary entry pressure measurements on Quest MCS core plugs suggested no CO_2 entry for capillary pressure less than 999 psi. At the capillary pressure higher than 999 psi, the measured flow rate was independent of the pressure drop. It indicated that the cap rock was extremely tight such that the fluid transport was not viscous flow, nor can it be described by Darcy's Law. Instead, the fluid transport was dominated by the diffusion process and the CO_2-brine-rock interaction.

SEM images obtained on the core sample RAW004 before and after SC CO_2 entry pressure measurement confirmed very tight pores with poor connectivity in the cap rock. Those images also revealed halite crystals along the edges of micro-cracks close to the inlet side, which were not observed on sample before the CO_2 test. XRD analysis showed the presence of calcite after the CO_2 test. The elemental study provided strong evidence on the SC CO_2-brine-rock interaction, including evaporation, dry-out, precipitation, and brine imbibition. More importantly, the presence of calcite and the variation in its amount along the core plug strongly suggested that diffusion was the dominant process for mass transfer inside the pore space. Precipitation of calcite reduces the CO_2 concentration, and may also serve as a barrier to the CO_2 diffusive flow.

The caprock study in this work demonstrated that there are strongly coupled physical and chemical processes between SC CO_2 and water saturated rock. Therefore integration of different measurements, analysis, and numerical modeling is a must for future cap rock integrity assessment. The following types of tests/analysis are strongly recommended: capillary entry pressure measurement, mineralogy, imaging and elemental analysis before and after entry pressure test, and composition analysis on water before and after entry pressure test.

6. Acknowledgement

The Spectroscopy and Microanalysis Team is acknowledged for performing SEM image and X-ray Diffraction Analysis. The authors would also like to thank David Denley, Guo-Xiang Zhang, Peter Doe, Xiao-Hui Xiao, and Zhe-Yi Chen for insightful discussion. David, Guo-Xiang, and Peter also reviewed the report. Their time is highly appreciated.

References

[1] M. Winkler, "Generation-4 Integrated Reservoir Modeling Report", AA5726 – Field Development Plan 07-3-AA5726-0001, Shell International Exploration and Production Inc., Houston, 2011

[2] A. Busch, "The Signifciance of Caprock Sealing Integrity for CO2 Storage", Shell Report, EP2010-5264, Shell International Exploration and Production B. V., Rijswijk, 2010.

[3] G. Zhang and M. Winkler, "Quest Cabron Capture and Storage: Geochemistry and Geochemical Reactive Transport Modeling", PPT for external review, Calgary, Canada, 2011.

[4] P. Chiquet, D. Broseta, and S. Thibeau, "Capillary Alteration of Shaly Caprocks by Carbon Dioxide", Soceity of Petroleum Engineers, SPE94183, 2005.

[5] D. B. Bennion and S. Bachu, "Dependence on Temperature, Pressure, and Salinity of the IFT and Relative Permeability Displacement Characteristics of CO2 Injected in Deep Saline Aquifers", Soceity of Petroleum Engineers, SPE102138, 2006.

[6] S. Li, M. Dong, Z. Li, S. Huang, H. Qing, and E. Nickel, "Gas Breakthrough Pressure for Hydrocarbon Reservoir Seal Rocks: Implications for the Security of Long-Term CO2 Storage in the Weyburn Field", Geofluids, 5, p326-334, 2005.

[7] A. Hildenbrand, S. Schlömer, and B. M. Krooss, "Gas Breakthrough Experiments on Fine-Grained Sedimentary Rocks", Geofluids, 2, p2-23, 2002.

[8] A. Hildenbrand, S. Schlömer, B. M. Krooss, and R. Littke, "Gas breakthrough experiments on pelitic rocks: comparative study with N2, CO2, and CH4", Geofluids, 4, p61-80, 2004.

[9] P. F. Boulin, P. Bretonnier, V. Vassil, A. Samouillet, M. Fleury, and J. M. Lombard, "Entry Pressure Measurements using Three Unconventional Experimental Methods", Society of Core Analysts International Symposium Proceedings, 2011-02, September 2011, Austin, USA.

[10] M. Carpita, T. Giorgis, and A. Battistelli, "Modeling CO2 Injection with Halite Precipitation using an Extended Verma & Pruess Porosity - Permeabiltiy Model", TOUGH Symposium Proceeding, May 2006, Lawrence Berkeley National Laboratory.

[11] C. Grattoni, P. Guise, G. Phillips, Q. Fisher, and R. Knipe, "Evaluation of Water Evaporation and Salt Precipitation due to Flow in Gas Reservoirs", Society of Core Analysts International Symposium Proceedings, 2009-14, September 2009, Noordwijk, The Netherlands.

[12] Y. Wang, E. Mackie, J. Rohan, T. Luce, R. Knabe, and M. Appel, "Experimental Study on Halite Precipitation during CO2 Squestration", Society of Core Analysts International Symposium Proceedings, 2009-25, September 2009, Noordwijk, The Netherlands.

[13] Y. Wang, T. Luce, C. Ishizawa, M. Shuck, K. Smith, H. Ott, and M. Appel, "Halite Precipitation and Permeability Assessment during Supercritical CO2 Core Flood", Society of Core Analysts International Symposium Proceedings, 2010-18, October 2010, Halifax, Canada.

[14] H. Ott, K. de Kloe, C. Taberner, F. Marcelis, Y. Wang, and A. Makurat, "Rock/Fluid Interaction by Injection of Supercritical CO2/H2S: Investigation of Dry-Zone Formation near the Injection Well", Society of Core Analysts International Symposium Proceedings, 2010-20, October 2010, Halifax, Canada.

[15] D. B. Bennion and S. Bachu, "Supercritical CO2 and H2S - Brine Drainage and Imbibition Relative Permeability Relationships for Intergranular Sandstone and Carbonate Formations", Society of Petroleum Engineers Conference Paper, SPE 99326, 2006..

Appendix 1.

This Appendix captures the capillary entry pressure measurements on a tight gas plug in 2008. It served as a basis to establish the measurement protocol. The setup consisted of a pressure confining core holder, a diaphragm, three displacement pumps, pressure transducers, and valves. All three pumps could inject or withdraw fluid at constant rate or under constant pressure. Note that for those displacement type pumps used in this work, volume changes were recorded in the opposite direction to that shown in Figure 2.1. Any production at the downstream side was indicated by the volume decrease in the back pump. A 10 cc diaphragm was used to separate CO_2 from the working fluid (Soltrol) of the injection pump. The whole setup was enclosed in a temperature controlled box and maintained at 50 °C during the test. A tight gas core plug sample was used to mimic the caprock. It had a porosity of 5% and permeability of 0.003 mD. The effective stress on the plug was 800 psi, and the back pressure was maintained at 1280 psi.

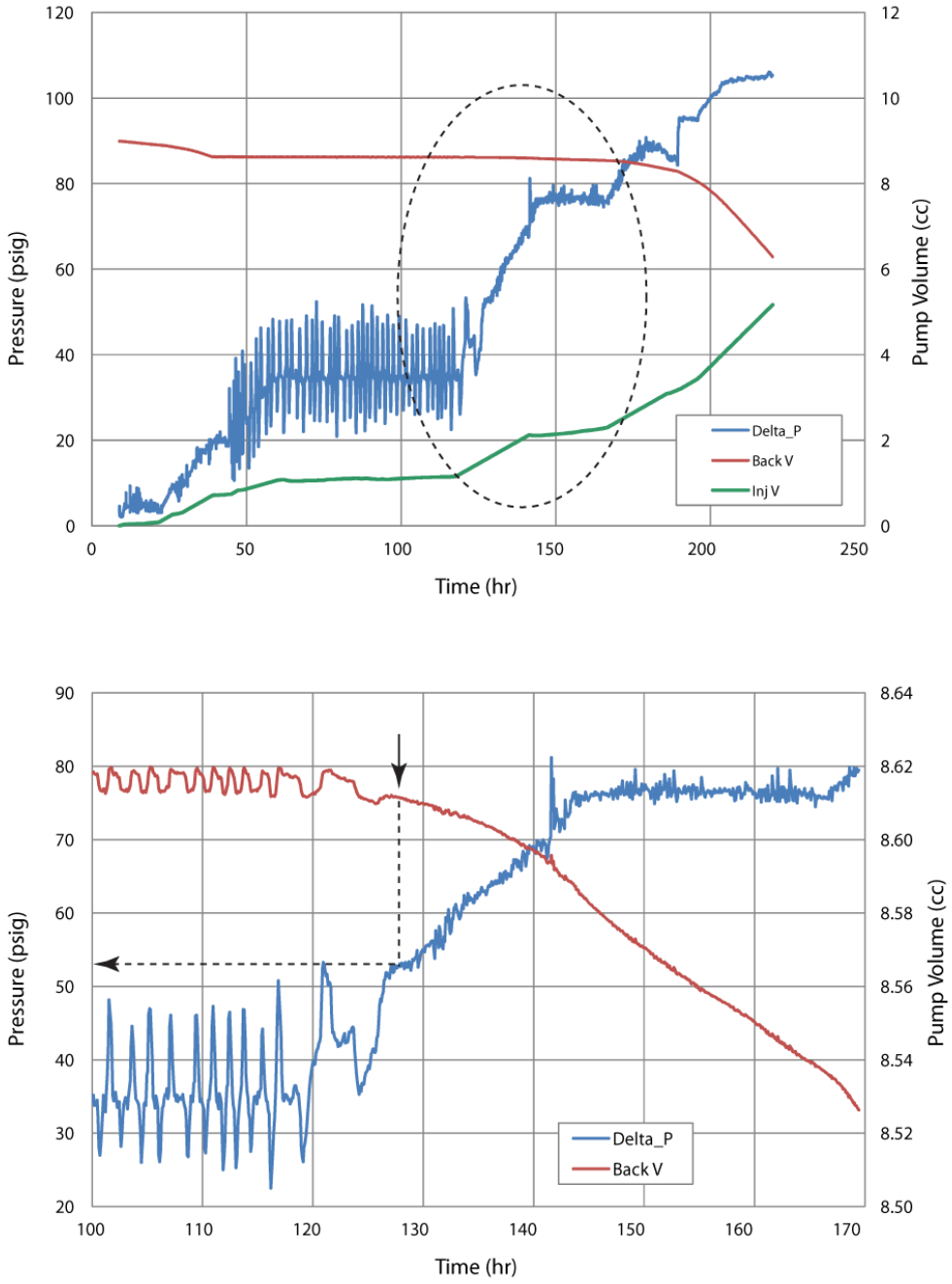

Figure A1.1: Delta pressure and pump volume changes during the SC CO_2 entry pressure measurement on a tight gas core plug (top chart), with the portion highlighted by dashed circle magnified in the bottom chart to show the CO_2 entry (indicated by arrows).

The capillary entry pressure was measured by a step-wise steady-state method as outlined below:

- The system was leak tested using a dry Berea core plug filled with dry SC CO_2 at about 1250 – 1300 psi and 800 psi effective stress for 7 days.
- The sample was vacuumed over 12 hours and saturated with 7% de-gased brine (the "dead brine"). The dead brine in the core plug was then displaced by "live brine" (7% brine saturated with CO_2 at 1215 psi and 50 °C) at a rate of 1 cc/day for about 5 pore volumes.
- After the live brine injection was finished and the back pressure was stabilized, dry SC CO_2 was injected at a rate of 1 cc/day while the back pressure was maintained at 1280 psi. The effective stress (confining pressure minus the injection pressure) was 800 psi.
- SC CO_2 was injected continuously until the preset pressure drop ($\Delta P = P_i - P_b$) across the sample was reached. Then the injection pump was switched to maintain that pressure drop automatically for 6 hours or longer.
- At each preset pressure drop, the volume change of the back pump was monitored and recorded. Entry pressure was determined from the back pump movement.

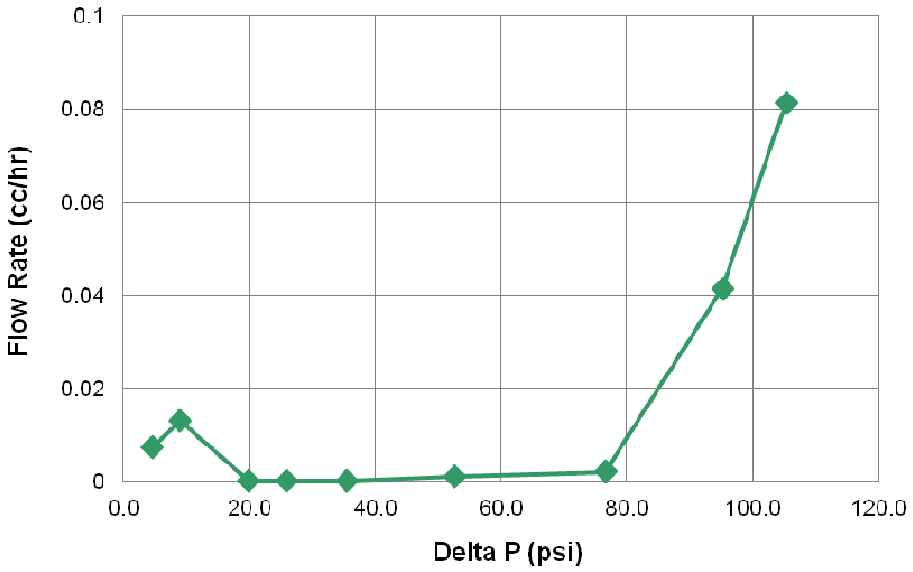

Figure A1.2: Flow rate at each delta pressure during the SC CO_2 entry pressure measurement on a tight gas core plug.

Figure A1.1 shows the pressure drop (ΔP) across the core plug, as well as volume changes in injection and back pumps during the measurement. Where ΔP was set at 4.5, 8.9, 19.8, 25.9, 35.5, 76.5, 95.2, and 105.2 psi, respectively. During the first 39 hours of the injection, SC CO_2 was displacing the brine in the upstream tubing and end-piece. The back pump moved slightly to accommodate the brine production. When the CO_2 front reached the top surface of the core plug at $t_{exp} \approx 39$ hr, $\Delta P = 19.8$ psi, the CO_2 pressure was lower than the capillary entry pressure. Therefore, no more brine was displaced and the back pump volume stopped changing. After that the CO_2 pressure was increased in steps. When $\Delta P < 53$ psi, no brine was produced and the back pump did not move. Fluctuations in the measured pressure were due to the unoptimized pump control parameters. The back pump started moving at $\Delta P = 53$ psi or $t_{exp} \approx 127$ hr, which indicated capillary entry. When $t_{exp} > 148$ hr and $\Delta P = 95.2$ psi, CO_2 flow path was fully established in the core plug.

The back pump started moving at the same rate as that of the injection pump. The movement in both pumps increased proportionally as the pressure drop increased to 105.2 psi (t_{exp} > 200 hr). The measured flow rate verses the pressure drop across the sample is plotted in Figure A1.2, where the flow rate was calculated from the back pump volume change. Figure A1.2 is the relation between pressure drop and the flow rate. It shows that after the CO_2 breakthough the flow rate was proportional to the pressure drop as described by Dary's Law.

After the above entry pressure experiment, a stressed mercury capillary pressure curve was measured on the same core plug. The measured mercury entry pressure was 775.6 psi. From interface tension (32 dyne/cm) and contact angle (θ = 45°) of SC CO_2 [4] [15], the corresponding SC CO_2 entry pressure calculated from the mercury entry pressure was 48 psi, which agreed reasonably with the measured value (53 psi).

Bibliographic information

Classification	Unrestricted
Report Number	SR.12.13365
Title	Capillary Sealing Capacity of Radway Middle Cambrian Shale Core Samples for Quest CCS Project
Author(s)	Yingxue Wang (PTU/ADD)
	Robert J. Knabe (PTI/RF)
Keywords	Capillary entry pressure, Quest MCS, CO2-brine-rock interaction
Date of Issue	October 2012
Period of Work	Oct. 2011 - Aug. 2012
US Export Control	US - Non Controlled (EAR99)
WBSE Code	ZZPT/015258/010301
Reviewed by	D. Denley (PTD/TASE)
	P. Doe (PTU/ADD)
	G. Zhang (PTU/DF)
Approved by	M. Appel (PTI/RF)
Sponsoring Company / Customer	SIEP. Inc,
Issuing Company	Shell International Exploration and Production Inc.
	Westhollow Technology Center
	3333 Highway 6 South
	Houston TX 77082-3101
	USA